Alexandria Engineering Journal 95 (2024) 376–393

Contents lists available at ScienceDirect

Alexandria Engineering Journal

journal homepage: www.elsevier.com/locate/aej

Fault detection in analog electronic circuits using fuzzy inference systems and particle swarm optimization

M.I. Dieste-Velasco

Electromechanical Engineering Department, Higher Polytechnic School, University of Burgos, 09006 Burgos, Spain

ARTICLE INFO

Keywords:
Analog electronic circuits
Fault diagnosis
Fault classification
Fuzzy inference systems (FIS)
Particle swarm optimization (PSO)
Pattern search

ABSTRACT

Fault detection in analog circuits is of great importance to predict the correct operation of the circuit. For this purpose, soft computing techniques such as those based on the application of fuzzy inference systems stand out. However, given the large variability that can exist in analog circuits due to component tolerance, the initial fuzzy inference system (FIS) may not be able to accurately diagnose the different hard faults. This study presents a methodology to diagnose and detect the faults that can occur in analog circuits, which is based on the development of a FIS, starting from a specific fault situation in the analog circuit, and subsequently on the optimization of the membership functions using an evolutionary algorithm so that the adjusted FIS can classify and predict different failure situations. To this end, the application of optimization techniques based on particle swarm optimization (PSO) will be analyzed to develop a FIS capable of predicting different faults. In addition, pattern search algorithm will also be analyzed. A Sallen-Key band-pass filter and a single stage of a small-signal amplifier are used as test circuits. The proposed methodology shows that it is possible to accurately predict the faults that could arise in the circuits under study.

1. Introduction

In analog electronic circuits it is very important to determine the possible faults in order to ensure the correct operation of these circuits, which is a more difficult and less developed task than in digital circuits [1]. Among the factors that make this task more difficult, it is worth mentioning that, in general, test points are not available to verify all the circuit's components. Moreover, it is not practical to perform measurements on each component. Therefore, it is necessary to use some kind of technique to predict circuit behavior in the event of a potential failure. One of the techniques that can be used is to select a set of measurement points and analyze the values obtained both when the circuit is operating at its nominal mode and when it is in a fault condition. Since, for practical reasons, it is not possible to measure all the components of the circuit, there will be faults that could cause several equivalent states, from the point of view of the measurements made on the circuit.

In recent years machine learning techniques have been widely used to detect and classify faults in analog electronic circuits as can be seen in the review by Mohd et al. [2] as well as in various engineering applications [3,4] because these powerful techniques allow efficient modeling and detection of faults. As is well known, machine learning focuses on the development of algorithms and statistical models that allow predictions to be made from input data [5]. On the other hand, some other techniques such as deep learning methods generally involve three or more layers of artificial networks and tend to be more complex models than those obtained by machine learning-based algorithms, such as support vector machines (SVM) or conventional artificial neural networks (ANN). Typical deep learning architectures include deep belief networks (DBN), autoencoders (AE), convolutional neural networks (CNN) and recurrent neural networks (RNN) [6]. Traditional neural learning methods, extract features manually, whereas deep learning methods automatically obtain feature representations by layer-by-layer feature transformation on original data usually via back-propagation [6]. Each method has its own strengths and weaknesses, and the best choice depends on the specific requirements of each task [5]. On the other hand, in fuzzy logic "if/then" rules allow to overcome the traditional two-valued logic expressions [7]. It is possible to model electronic circuits with different levels of complexity. However, the relationship between membership functions and fuzzy rules must be determined [7]. Depending on the problem being analyzed, one approach may be preferable to the other.

With regard to analog electronic circuits, as can be seen in research studies such as that of Shi et al. [8] the authors used Monte Carlo simulations and a dynamic weight probability neural network for fault

E-mail address: midieste@ubu.es.

https://doi.org/10.1016/j.aej.2024.01.054
Received 6 October 2023; Received in revised form 15 December 2023; Accepted 17 January 2024
Available online 17 April 2024

diagnosis. Machine learning combined with Monte Carlo analysis was also used by Arabi et al. [5] for soft faults detection and classification in analog electronic circuits. Likewise, Zhang et al. [9] employed unsupervised clustering combined with electronic simulation to detect faults in analog electronic circuits. Further examples are that of Xiao and He [10] that employed simulation to develop an approach based on wavelet and neural networks for fault classification; that of Zhang et al. [11] that employed an improved wavelet transform-based features extraction and multiple kernel extreme learning machine-based diagnosis model for analog circuit fault diagnosis, and that of Sheikhan et al. [12] that employed a modular ANN and particle swarm optimization to detect soft faults in analog circuits. Similarly, In Dieste-Velasco [13] a pattern recognition ANN was employed and in Zhong et al. [14] deep belief neural networks were employed to detect intermittent faults that may arise in this kind of circuits.

There are two main approaches to fault detection in analog electronic circuits: simulation before test (SBT) and simulation after test (SAT). In SAT, the methods mainly focus on parameter identification and in SBT the outputs of the circuit under test (CUT) are compared with the stored values in a fault dictionary to detect the faults. In the SBT method the main faults and the nominal behavior are usually simulated. In addition, it is also very important to determine the ambiguity groups, i.e., the set of components that have no single solution when considered as a possible failure, as shown in Aizenberg et al. [15].

Among the research studies dealing with the application of fuzzy logic for fault detection in analog circuits, it is worth mentioning that one developed by Arabi et al. [16] who used frequency and transient responses for fault classification by using an adaptive-network-based fuzzy inference system (ANFIS). The results of their study were also compared with those obtained by artificial neural networks (ANN), where they obtained higher accuracy with the ANFIS classification. A statistical analysis of the frequency response of analog circuits and fuzzy logic was also used to detect and identify faulty components in the study of Nasser et al. [17]. Further examples are that of He et al. [18] that employed a hybrid approach combining cross-wavelet transform, Bayesian matrix factorization, and support vector machine for fault diagnosis of analog circuits; Cui et al. [19] that employed fuzzy logic to detect hard faults in analog electronic circuits and that of Li and Xie [20] who used the cross-entropy between a circuit under nominal behavior and another one with faults along with Monte Carlo simulation, in order to diagnose faults in the circuit. In addition, He et al. employed a PSO-SVM classifier to locate faults in electronic circuits [21]. Further studies are those of Yang et al. [22] where a model to identify multiple faults in analog electronic circuits was developed. In Zuo et al. [7] subtractive clustering was used to determine the initial structure of the ANFIS fault diagnosis model and then wavelet techniques were used to extract fault characteristics of the circuit where four faults were considered as well as the nominal behavior. Similarly, in Khalid et al. [23] a PSO optimized subtractive clustering was used to develop and train an ANFIS for fault detection.

Some other studies are that of Kumar et al. [24] where soft faults are diagnosed using a fuzzy classifier, and that of Yu et al. [25] who employed firefly algorithm and machine learning combined with simulation by Monte Carlo analysis to detect faults in analog electronic circuits, where a Sallen-Key was used as CUT. Supervised learning was also used in Parai et al. [26] to detect soft faults in analog electronic circuits,. where three types of active filters were employed in their study as CUTs. Moreover, these authors used Monte Carlo simulation from tolerances of the circuit components [26].

Further examples can be found in He et al. [27] who used cross wavelet transform (XWT), bilateral 2D linear discriminant analysis (B2DLDA) and vector valued regularized Kernel function approximation (VVRKFA) for fault diagnosis in analog circuits. In addition, these authors employed QPSO as the tuning algorithm. Likewise, these authors employed simulation and the results obtained showed that high accuracy was achieved.

On the other hand, Bilski [28] employed both supervised and unsupervised learning to detect faults in analog electronic circuits and Zhao et al. [29] used deep belief networks combined with Monte Carlo analysis and time domain signal sampling, among many others.

This present study shows a methodology to diagnose and detect the faults that can occur in analog circuits, which is based on the development of a FIS, starting from a specific fault situation in the analog circuit, and subsequently on the optimization of the parameters of the membership functions by using an evolutionary algorithm, so that the adjusted FIS can classify and predict the events that precede the actual hard fault, which is important because the outputs obtained after the hard fault has occurred may be different from others that precede the actual fault. In order to diagnose fault events that are relatively close to the actual hard fault but may have different outputs from the point of view of the measurement points, a Monte Carlo analysis of the component tolerance was performed. As shown in the review by Binu et al. [30], most of the hard faults that can occur in analog electronic circuits are caused by open and short circuits, where these faults can be modeled by including a series resistor and a parallel resistor, respectively, along with the faulty component. Therefore, in the present study, this modeling is used to obtain different inputs from the component tolerance by using a Monte Carlo analysis and the corresponding outputs in the measurement points. It should be mentioned that despite the fact that fuzzy logic has been used for fault detection in recent years, these fuzzy inference systems (FISs), developed from the initial analysis of the circuit configuration, are usually not optimized to predict events other than those analyzed to develop the original FIS. Therefore, due to the variability that may exist in the circuit, the original FIS may not be able to accurately predict different fault situations. The current study presents a methodology based, first, on the development of a FIS from the analog electronic circuit configuration in the actual hard fault situation. Second, once this initial FIS is obtained, it is then adjusted to detect the faults that may arise prior to the actual hard faults.

2. Proposed method

In order to develop the initial FIS, the number of measurements to be taken in the circuit to characterize the hard faults should be chosen. Therefore, in the event of a hard fault, the CUT is first analyzed from the nominal values of the components. Once the outputs of the circuit are determined, it is necessary to select the number of them to characterize the possible faults in the CUT. Because fault configurations can occur that produce ambiguous outputs, making it impossible to determine exactly which component is failing, identifying these fault situations is a previously necessary task. Therefore, the number of fault classes corresponding to each variable should be selected. Moreover, if the number of classes thus obtained is to be increased, then an increase in the number of measurements to be made on the outputs could be considered, in order to be able to identify the hard faults in the circuit more precisely, as shown in the flowchart depicted in Fig. 1. On the other hand, the outputs of the CUTs, both in nominal behavior and in actual hard fault conditions, could be affected by changes in the tolerances of the circuit components. Therefore, once the initial FIS is obtained, the CUTs outputs are analyzed to determine its performance. For this purpose, single hard faults due to short circuits and open circuits were obtained by using Cadence®OrCAD® from Monte Carlo analysis. Once these values were obtained, Matlab™2022a as well as the Fuzzy Logic Toolbox™ of Matlab™[31] were employed to develop the FIS. However, this FIS may not be able to accurately predict the hard faults that can occur in the CUT and hence, as shown in Fig. 1, some optimization algorithm has to be employed to adjust the membership functions (MFs) in order to increase the accuracy. It will be shown later in this study that the adjusted FIS is able to detect the faults that can occur in the CUTs both in actual hard faults and in situations preceding hard faults, which are characterized by the above-mentioned modeling.

A zero-order Sugeno FIS [32] was selected and Gaussian MFs were

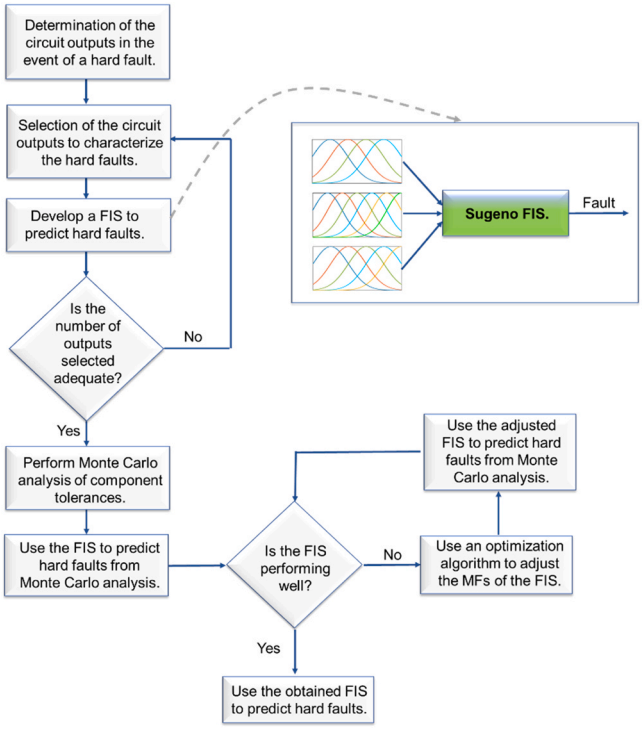

Fig. 1. Flowchart of the proposed methodology.

used for the inputs, as Eq. (1) shows. However, it is worth mentioning that any other type of membership functions could have been used such as triangular, bell-shaped, etc. As is well known, a type-1 fuzzy set may be defined as a set of function on a universe X, as Eq. (2) shows, where the membership of A is denoted as $\mu_A(x)$ [31,33].

$$\mu(x) = e^{\frac{-(x-m)^2}{2\sigma^2}} \tag{1}$$

$$A = \{(x, \mu_A(x))|_{x\in X},\ where\ 0 \le \mu_A(x) \le 1\} \tag{2}$$

Therefore, the FIS developed for modeling the behavior of the CUTs have a set of rules given by Eq. (3).

$$If\ \left(Input_1\ is\ I_{1,i}\right)\&...\&\left(Input_n\ is\ I_{n,k}\right)\ then\ \left(Output\ is\ Fault\ class_m\right) \tag{3}$$

Eq. (4) shows the implication method, and the FIS output is shown by Eq. (5).

$$w_j(x) = \text{AndMethod}\left\{\mu_{j1}(x_1), \ldots, \mu_{jn}(x_n)\right\} \tag{4}$$

$$F = \frac{\sum_{j=1}^{Number\ of\ rules} w_j * F_j}{\sum_{j=1}^{Number\ of\ rules} w_j} \tag{5}$$

The set of rules shown in Eq. (3) were obtained from the actual hard faults that may arise in the CUTs. Since the defuzzification is computationally more efficient in Sugeno FIS [31,34], this kind of FIS was used in this study. In order to obtain this FIS, the potentially faulty components were short-circuited and open-circuited. After identifying the output values, the faults with an ambiguous configuration (fault classes) were selected. From this, a set of inputs was generated to develop the FIS and the corresponding outputs were the possible fault classes and the nominal behavior, so that the fault classes as well as the nominal behavior were determined by the values of the input variables, according to Eq. (3). From the measured values of the inputs, it was then possible to determine the number of membership functions corresponding to each of them.

As previously mentioned, Gaussian membership functions as shown in Eq. (1) were used. In order to select the parameters of these membership functions, the values obtained from the hard faults were employed. This makes the zero-order Sugeno FIS adequately predict the hard faults (characterized by actual open circuits and short circuits in the components). However, as will be shown afterwards, this initial FIS is not capable of predicting events close to the actual hard faults. Therefore, in order to increase the accuracy of the initial FIS, an optimization algorithm should be used to optimize the parameters of the membership functions in order to predict both the actual hard faults as well as those events near to the hard faults. For this purpose, open circuits (oc) were simulated by connecting a resistor in series with the faulty components and short circuits (sc) were simulated by connecting a resistor in parallel with the faulty components. To generate different faults, the tolerances of the circuit components were used to perform a Monte Carlo analysis on each of the possible faults in order to determine the variability that may exist in the test points of the analog circuits. In this study, 64 Monte Carlo runs were considered for each of the possible faults and also for the nominal behavior and supervised learning was employed. In addition, the FIS outputs were not changed during the tuning, as these values corresponded to the nominal behavior and to the fault classes.

In order to adjust the membership functions, different optimization alternatives could be selected. In this study, particle swarm optimization (PSO) and pattern search were considered to determine the optimization algorithm that provided the best results. Two analog electronic circuits were considered as CUTs in order to demonstrate the performance of the obtained FIS: a second-order Sallen-Key band-pass filter and a BJT amplifier.

3. Simulation results and discussion

The results obtained with the two selected CUTs and a discussion of them are shown in this Section.

3.1. Analysis of the Sallen-Key circuit

A Sallen-Key bandpass filter as shown in Fig. 2 was first analyzed. Standard commercial components were selected. In this case, tolerances were considered to be 10%, which is a very high value for the filter, making it more difficult to detect faults. Fig. 3 depicts the frequency response of the filter shown in Fig. 2 at the different hard faults (short circuits and open circuits) and at the nominal behavior.

From the plots shown in Fig. 3 it would be possible to select some frequencies in order to determine the voltage outputs to develop the FIS. In addition, all the values shown in Fig. 3 were plotted together in Fig. 4 in order to show the difficulty of selecting a specific frequency to develop the FIS, since several of the outputs provide similar results. As a first step, two frequencies were selected, one close to the nominal

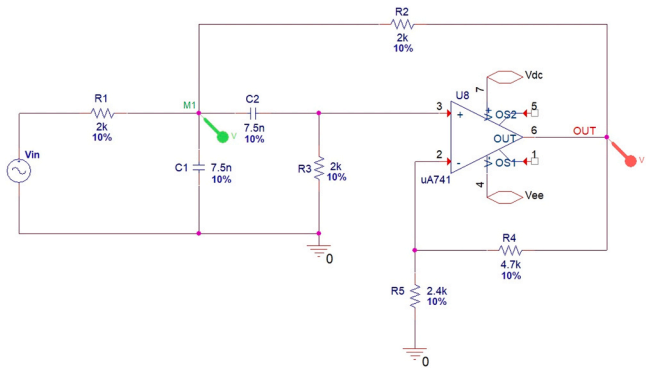

Fig. 2. Electrical diagram of the Sallen-Key band-pass filter employed as CUT.

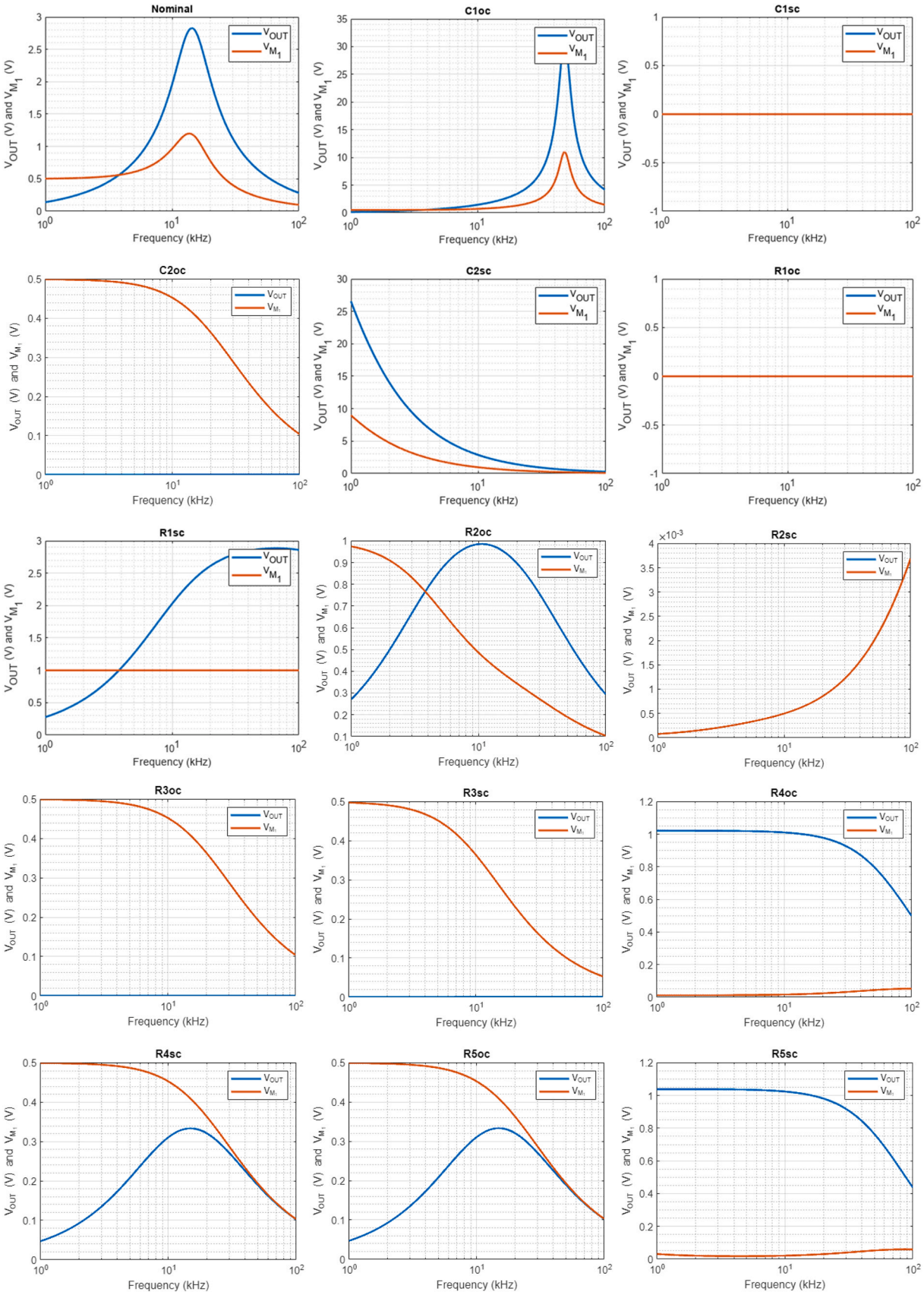

Fig. 3. Frequency response of the Sallen-Key Circuit at the selected points M1 and OUT.

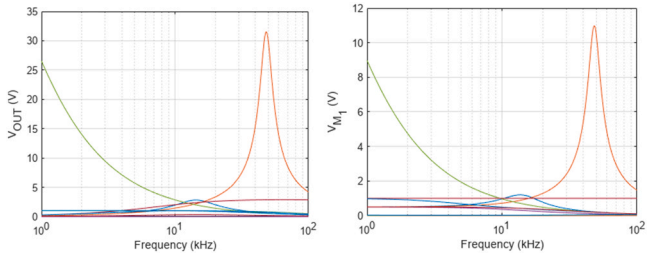

Fig. 4. Frequency response of the Sallen-Key Circuit at the M1 and OUT for all faults.

Table 1
Fault classes for the Sallen-Key band-pass filter grouped by ambiguity groups with two measurements of V_{OUT} (V) at two different frequencies.

Fault class	Fault	Name	V_{OUT_1}	V_{OUT_1j}	V_{OUT_2}	V_{OUT_2j}
FC_{02}	F_{03}	C_{1sc}	0.0000	1	0.0000	1
FC_{02}	F_{06}	R_{1oc}	0.0000	1	0.0000	1
FC_{02}	F_{09}	R_{2sc}	0.0007	1	0.0018	1
FC_{02}	F_{11}	R_{3sc}	0.0003	1	0.0004	1
FC_{02}	F_{04}	C_{2oc}	0.0005	1	0.0007	1
FC_{02}	F_{10}	R_{3oc}	0.0002	1	0.0001	1
FC_{03}	F_{13}	R_{4sc}	0.3334	2	0.2058	2
FC_{03}	F_{14}	R_{5oc}	0.3334	2	0.2058	2
FC_{04}	F_{08}	R_{2oc}	0.9589	3	0.5870	3
FC_{05}	F_{12}	R_{4oc}	0.9976	3	0.8377	4
FC_{05}	F_{15}	R_{5sc}	1.0057	3	0.8033	4
FC_{06}	F_{05}	C_{2sc}	1.9043	4	0.6324	3
FC_{07}	F_{02}	C_{1oc}	2.3146	5	26.5286	6
FC_{08}	F_{07}	R_{1sc}	2.4157	5	2.8631	5
FC_{01}	F_{01}	Nominal	2.8015	6	0.6812	3

Table 2
Fault classes for the Sallen-Key band-pass filter grouped by ambiguity groups with two measurements of V_{M1} (V) and V_{OUT} (V) at the same frequency.

Class	F	Name	V_{M1}	V_{M1j}	V_{OUT_1}	V_{OUT_1j}
FC_{02}	F_{03}	C_{1sc}	0.0000	1	0.0000	1
FC_{02}	F_{06}	R_{1oc}	0.0000	1	0.0000	1
FC_{02}	F_{09}	R_{2sc}	0.0007	1	0.0007	1
FC_{03}	F_{11}	R_{3sc}	0.2884	3	0.0003	1
FC_{04}	F_{04}	C_{2oc}	0.4081	4	0.0005	1
FC_{04}	F_{10}	R_{3oc}	0.4081	4	0.0002	1
FC_{05}	F_{13}	R_{4sc}	0.4080	4	0.3334	2
FC_{05}	F_{14}	R_{5oc}	0.4080	4	0.3334	2
FC_{06}	F_{12}	R_{4oc}	0.0189	2	0.9976	3
FC_{06}	F_{15}	R_{5sc}	0.0246	2	1.0057	3
FC_{07}	F_{08}	R_{2oc}	0.3970	4	0.9589	3
FC_{08}	F_{05}	C_{2sc}	0.6442	5	1.9043	4
FC_{09}	F_{02}	C_{1oc}	0.9582	6	2.3146	5
FC_{09}	F_{07}	R_{1sc}	1.0000	6	2.4157	5
FC_{01}	F_{01}	Nominal	1.1597	7	2.8015	6

frequency of the circuit and the other one three times higher than the nominal frequency.

The voltage results obtained for each fault are shown in Table 1, where V_{OUT_1} and V_{OUT_2} correspond to the measurements taken at the nominal frequency and at a frequency three times higher than the nominal one, respectively. Likewise, V_{OUT_1j} and V_{OUT_2j} correspond to the membership functions that are considered to develop the FIS. It should be noted that fault class number one (FC_{01}) does not correspond to a fault in the circuit, but to the nominal behavior. As can be seen in Table 1, only eight classes can be correctly distinguished from these two outputs since similar values are obtained. Therefore, a new possibility is considered in order to increase the number of fault classes, as shown in Table 2. In this second case, two measurement points were selected (V_{M1} and V_{OUT}), where the measurements were taken at the nominal frequency.

As can be seen in Table 2, it is possible to detect an additional fault class with these measurements. V_{M1} and V_{OUT_1} correspond to the measurements taken at the nominal frequency at both the input and output, respectively. Likewise, V_{OUT_1j} and V_{M1j} correspond to the membership functions that were considered to develop the second FIS.

Finally, Table 3 shows the outputs selected for the present study where two measurements were made at the nominal frequency of the filter, at points M1 and OUT, and an additional measurement was made at the output and at a frequency three times higher than the nominal one. In this latter case, it was possible to detect ten classes of faults. Given the characteristics of the circuit and the small number of measurements that have been used, there will be equivalent classes, i.e. they give the same output. The proposed method is a simple and fast method to implement, but it requires some faults to be classified into fault classes. Increasing the number of faults that the method can diagnose is possible, but it would also increase the complexity of the detection method and the number of features required to characterize the faults. Consequently, in the present study a small number of measurements was considered in order to simplify the process of extracting features from the circuit. Therefore, from the values shown in Table 3 was then possible to determine the nominal class and the fault classes shown in Table 4, which were grouped by ambiguity groups. From these values, a Sugeno FIS was first developed.

As previously mentioned, Gaussian memberhip functions were used in this study. Table 3 shows the values of these membership functions, that were obtained by averaging the values within the same fault class and using a standard deviation of $\sigma^2 = (k^*\overline{V_j})^2$, where k was taken as 10% and $\overline{V_j}$ were the average values of those shown in Table 3, within the same fault class. It should be noted that any other value of k could have been used. The resulting membership functions are shown in Fig. 5. These membership functions were obtained from Eq. (6).

Table 3
Fault classes for the Sallen-Key filter grouped by ambiguity groups with two measurements of V_{M1} (V) and V_{OUT} (V) at the nominal frequency and with an additional measurement of V_{OUT} (V) at a frequency three times higher than the nominal frequency.

Class	F	Name	V_{M1}	V_{M1j}	V_{OUT_1}	V_{OUT_1j}	V_{OUT_2}	V_{OUT_2j}
FC_{02}	F_{03}	C_{1sc}	0.0000	1	0.0000	1	0.0000	1
FC_{02}	F_{06}	R_{1oc}	0.0000	1	0.0000	1	0.0000	1
FC_{02}	F_{09}	R_{2sc}	0.0007	1	0.0007	1	0.0018	1
FC_{03}	F_{11}	R_{3sc}	0.2884	3	0.0003	1	0.0004	1
FC_{04}	F_{04}	C_{2oc}	0.4081	4	0.0005	1	0.0007	1
FC_{04}	F_{10}	R_{3oc}	0.4081	4	0.0002	1	0.0001	1
FC_{05}	F_{13}	R_{4sc}	0.4080	4	0.3334	2	0.2058	2
FC_{05}	F_{14}	R_{5oc}	0.4080	4	0.3334	2	0.2058	2
FC_{06}	F_{12}	R_{4oc}	0.0189	2	0.9976	3	0.8377	4
FC_{06}	F_{15}	R_{5sc}	0.0246	2	1.0057	3	0.8033	4
FC_{07}	F_{08}	R_{2oc}	0.3970	4	0.9589	3	0.5870	3
FC_{08}	F_{05}	C_{2sc}	0.6442	5	1.9043	4	0.6324	3
FC_{09}	F_{02}	C_{1oc}	0.9582	6	2.3146	5	26.5286	6
FC_{10}	F_{07}	R_{1sc}	1.0000	6	2.4157	5	2.8631	5
FC_{01}	F_{01}	Nominal	1.1597	7	2.8015	6	0.6812	3

Table 4
Fault classes for the Sallen-Key filter grouped by ambiguity groups.

FC_{01}	FC_{02}	FC_{03}	FC_{04}	FC_{05}	FC_{06}	FC_{07}	FC_{08}	FC_{09}	FC_{10}
F_{01}	{F_{03}, F_{06}, F_{09}}	F_{11}	{F_{04}, F_{10}}	{F_{13}, F_{14}}	{F_{12}, F_{15}}	F_{08}	F_{05}	F_{02}	F_{07}
Nominal	{C_{1sc}, R_{1oc}, R_{2sc}}	R_{3sc}	{C_{2oc}, R_{3oc}}	{R_{4sc}, R_{5oc}}	{R_{4oc}, R_{5sc}}	R_{2oc}	C_{2sc}	C_{1oc}	R_{1sc}

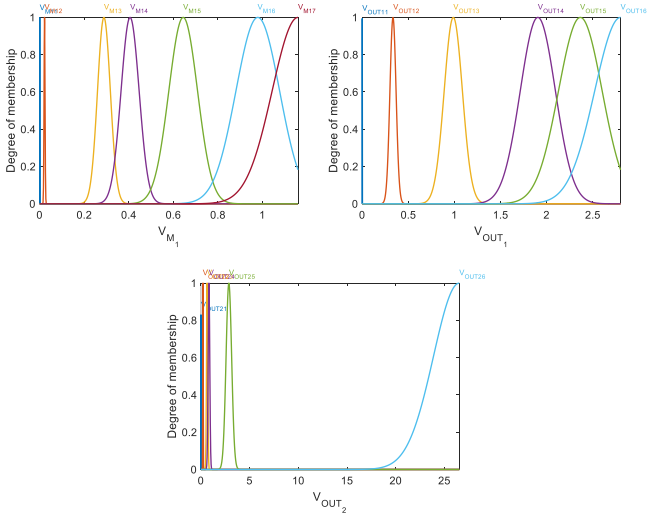

Fig. 5. Membership functions for classifying the faults in the S-K circuit.

$$\mu(x) = e^{\frac{-(x-\overline{V_j})^2}{2(k*\overline{V_j})^2}} \tag{6}$$

Likewise, the Sugeno FIS rules are shown in Table 5. As can be observed, the fault classes correspond to the nominal behavior and to the hard faults, where x1 and x2 correspond to V_{M1}, an V_{OUT} at the nominal frequency and x3 corresponds to V_{OUT} at three times the nominal frequency.

Fig. 6 shows the rule inference of the Sugeno FIS for the specific case of fault class number nine, which is an open circuit in capacitor C_1. As can be seen, the initial Sugeno FIS is able to accurately identify this fault.

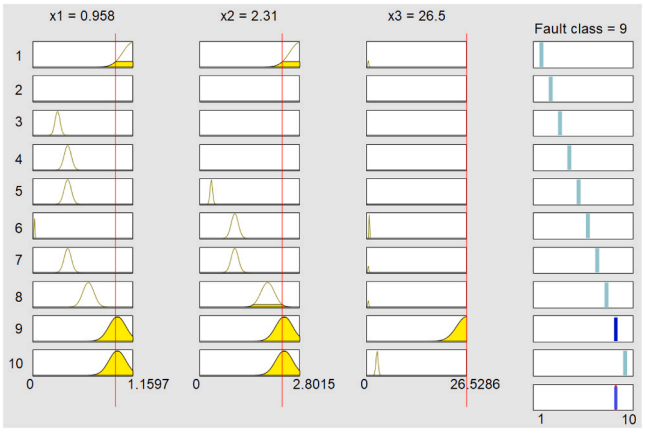

Fig. 6. Rule inference of the initial Sugeno FIS.

In addition, the initial Sugeno FIS developed in this way can accurately detect all fault classes. However, additional data is needed to analyze the performance of the FIS prior to the hard fault, as the FIS may not be able to diagnose these earlier situations with the same accuracy. Therefore, in order to have data available for this purpose, a new Monte Carlo analysis of the component tolerance was performed. This analysis resulted in different values of the measurement points for the output and input of the filter as shown in Fig. 7 and in Fig. 8, respectively. As can be observed, these plots are different from those obtained on the actual hard faults used to develop the initial Sugeno FIS, and therefore it is likely that the FIS developed in this way will not be able to accurately predict all possible faults. As will be shown below, this initial FIS is not capable of accurately predicting all of these results corresponding to hard faults, and therefore it is necessary to use an optimization algorithm in order to adjust the initial memberships as shown in Fig. 1.

Table 5
Rules and membership functions of the initial Sugeno FIS.

Membership functions for the inputs	Rules
[Input1]	1 "x1 ==x17 & x2==x26 & x3==x33 = > Fault class= 1″
'x11':'gaussmf',[2.333e-05 2.333e-04]	2 "x1==x11 & x2==x21 & x3==x31 = > Fault class= 2″
'x12':'gaussmf',[0.002175 0.02175]	3 "x1==x13 & x2==x21 & x3==x31 = > Fault class= 3″
'x13':'gaussmf',[0.02884 0.2884]	4 "x1==x14 & x2==x21 & x3==x31 = > Fault class= 4″
'x14':'gaussmf',[0.040584 0.40584]	5 "x1==x14 & x2==x22 & x3==x32 = > Fault class= 5″
'x15':'gaussmf',[0.06442 0.6442]	6 "x1==x12 & x2==x23 & x3==x34 = > Fault class= 6″
'x16':'gaussmf',[0.09791 0.9791]	7 "x1==x14 & x2==x23 & x3==x33 = > Fault class= 7″
'x17':'gaussmf',[0.11597 1.1597]	8 "x1==x15 & x2==x24 & x3==x33 = > Fault class= 8″
[Input2]	9 "x1==x16 & x2==x25 & x3==x36 = > Fault class= 9″
'x21':'gaussmf',[2.833e-05 2.833e-04]	10 "x1==x16 & x2==x25 & x3==x35 = > Fault class= 10"
'x22':'gaussmf',[0.03334 0.3334]	
'x23':'gaussmf',[0.09874 0.9874]	
'x24':'gaussmf',[0.19043 1.9043]	
'x25':'gaussmf',[0.236515 2.36515]	
'x26':'gaussmf',[0.28015 2.8015]	
[Input3]	
'x31':'gaussmf',[5e-05 5e-04]	
'x32':'gaussmf',[0.02058 0.2058]	
'x33':'gaussmf',[0.063353 0.63353]	
'x34':'gaussmf',[0.08205 0.8205]	
'x35':'gaussmf',[0.28631 2.8631]	
'x36':'gaussmf',[2.65286 26.5286]	

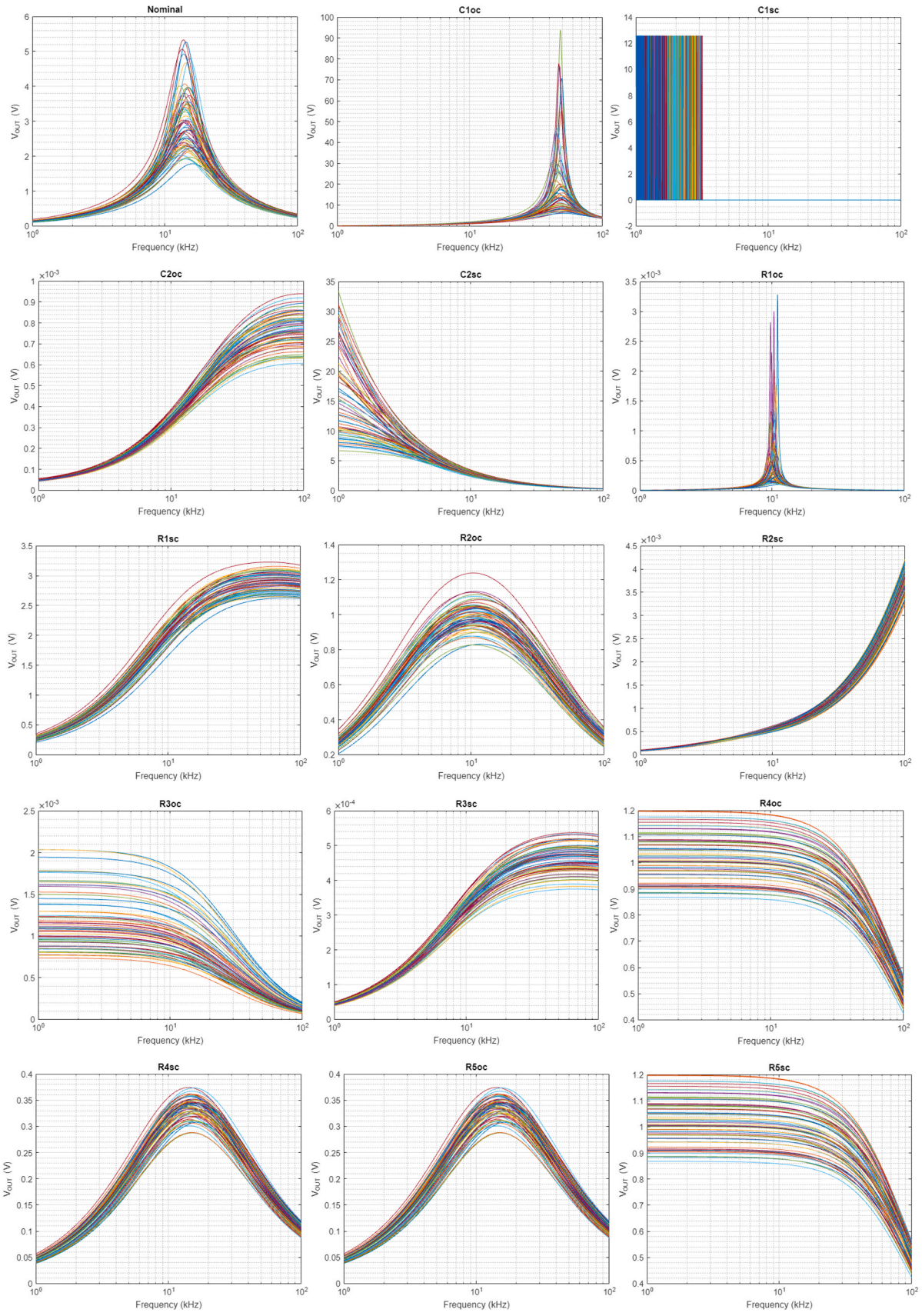

Fig. 7. Monte Carlo analysis from the tolerances of the resistors and capacitors of the circuit at the output. Observed values (V_{OUT}).

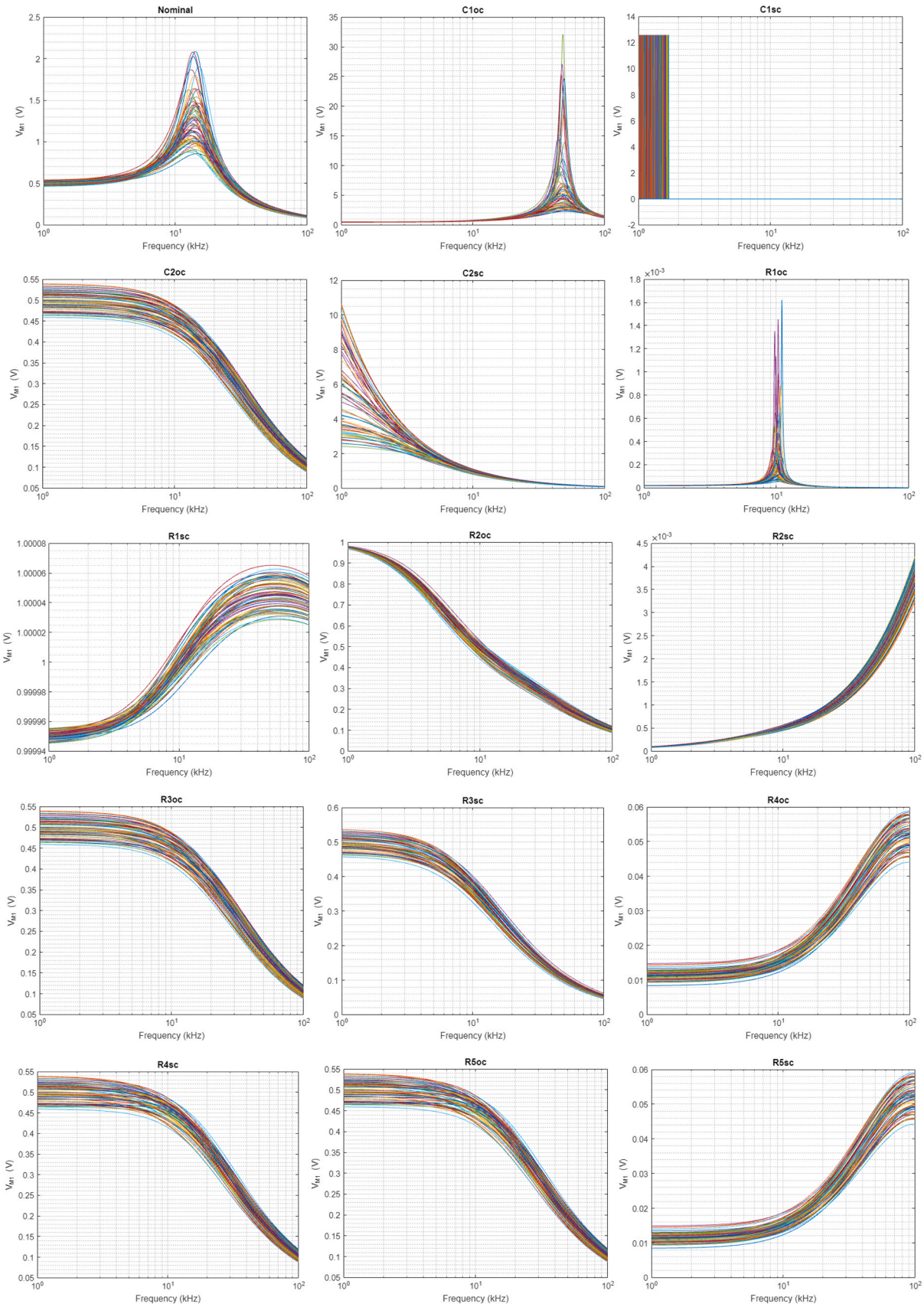

Fig. 8. Monte Carlo analysis from the tolerances of the resistors and capacitors of the circuit. Observed values (M1).

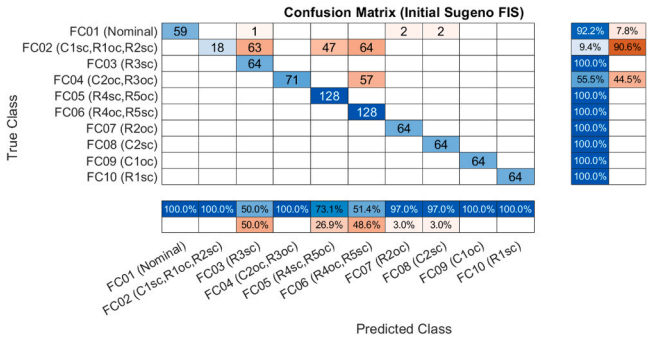

Fig. 9. Confusion matrix of the initial Sugeno FIS for predicting the faults using the Monte Carlo analysis data.

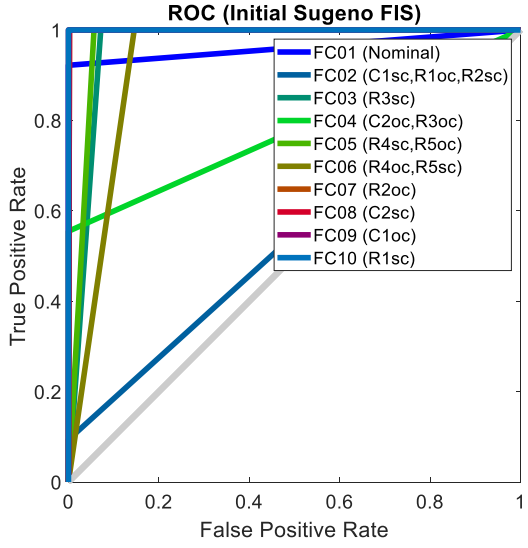

Fig. 10. ROC curve of the initial Sugeno FIS for predicting the faults in the S-K CUT.

From this Monte Carlo analysis, it was possible to obtain the inputs (V_{M1} and V_{out}) at the test points shown in Fig. 2. This analysis was carried out from the tolerances of the resistors and capacitors of the circuit shown in Fig. 2 for each of the hard faults. To carry out this Monte Carlo analysis, the hard faults were modeled by connecting a 0.1 Ω parallel resistor to the component (short circuit) and by connecting a 100 MΩ series resistor to the component (open circuit) with the aim of obtaining a higher variability than that obtained by performing a Monte Carlo analysis on the actual hard faults. The Monte Carlo analysis produced 64 results for each fault and for the nominal behavior. As previously mentioned, the tolerances were considered to be 10% which is a very high value and causes the center frequency of the filter to shift away from the nominal frequency, making the detection of hard faults a challenging task.

The initial Sugeno FIS was first used to predict the possible hard faults that were obtained from the Monte Carlo analysis. This was done by using the FIS to evaluate all the voltage measurements provided by the Monte Carlo results and by using the Matlab™ functions, i.e., "*evalfis (fisin,[x1,x2,x3])*" where [x1,x2,x3]= [V_{M1},V_{OUT1},V_{OUT2}] is an array (960 ×3) containing the Monte Carlo results. As can be seen, in the confusion matrix shown by Fig. 9, the initial Sugeno FIS was not able to accurately predict all the fault classes. Although seven fault classes were 100% detected only two of them were correctly predicted, i.e. there were no misclassified data, (FC_{09} and FC_{10}). As can be noted, for example, when FC_{03} occurs (true class), the predicted value is FC_{03}, so the value obtained in the right classification bar is 100%. However, there were some other values that were also predicted by the initial FIS as FC_{03} and did not correspond to this class as can be observed in the lower classification bar, where 63 values corresponding to class FC_{02} and 1 value of the nominal class were misclassified as FC_{03}. A similar behavior was observed for the fault classes (FC_{05}, FC_{06}, FC_{07} and FC_{08}). On the other hand, the nominal class was not correctly predicted by the initial FIS. It can be observed that 7.8% of the circuits that perform correctly were classified as having a fault.

On the other hand, both the class FC_{02} and the class FC_{04} were not correctly predicted by the initial FIS. This can also be observed in the Receiver Operating Characteristic curve (ROC curve) shown in Fig. 10 and also in Fig. 11, which shows all the inputs and the outputs of the FIS, that is, the predicted values.

Therefore, an optimization algorithm should be used, as previously mentioned in the flowchart shown in Fig. 1, to improve the accuracy of the initial Sugeno FIS. First, a particle swarm optimization (PSO) algorithm implemented in Matlab™2022 was used, which in turn is based on that of Kennedy and Eberhart [35] as shown in [36]. A description of the algorithm can be found in [35,37].

Fig. 12 shows the adjusted membership functions of the initial FIS using PSO. As can be observed from the confusion matrix shown by Fig. 13, the new adjusted FIS significantly improves the detection of faults in the S-K filter, not only those obtained from the actual hard

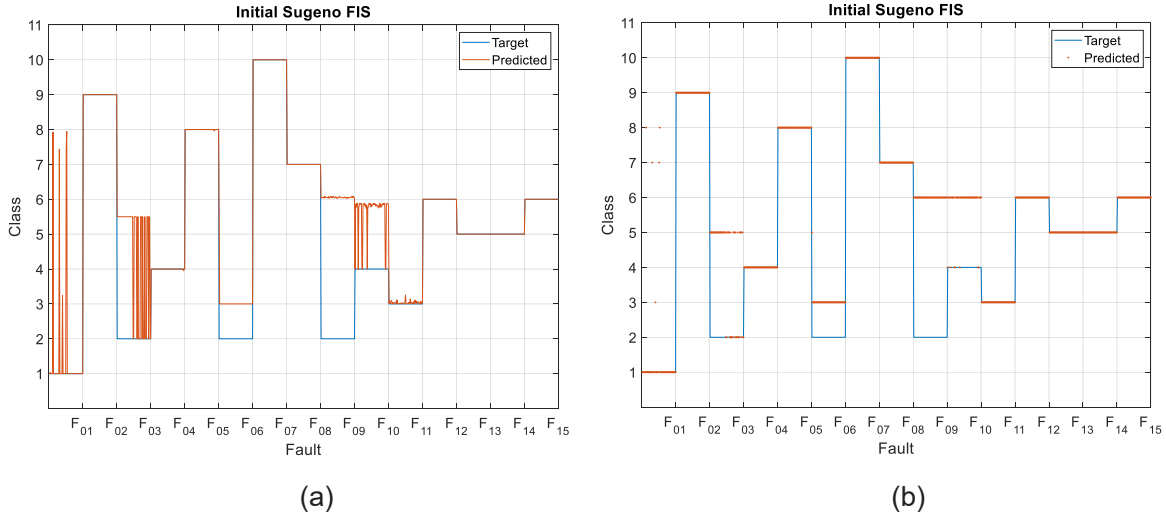

Fig. 11. Output of the initial FIS (a) actual output values and (b) output values rounded to the nearest integer.

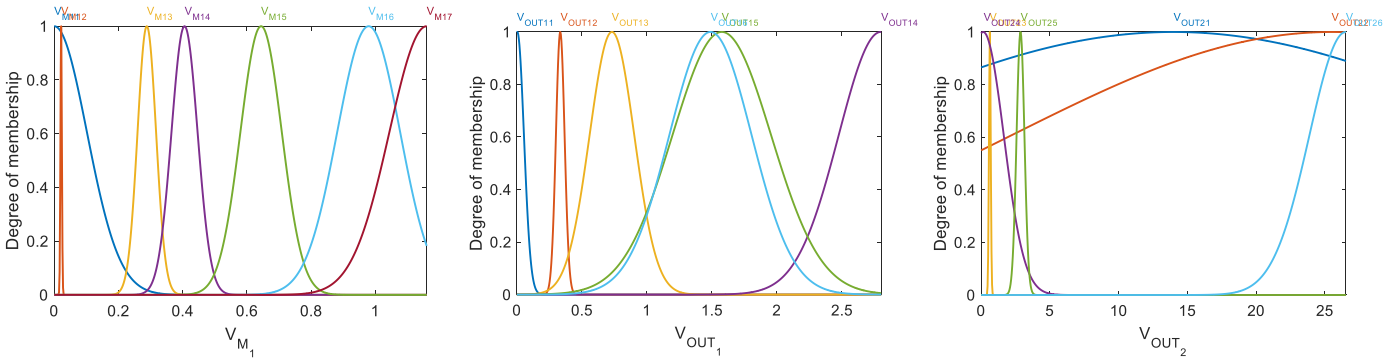

Fig. 12. Membership functions for classifying the faults in the S-K circuit after PSO.

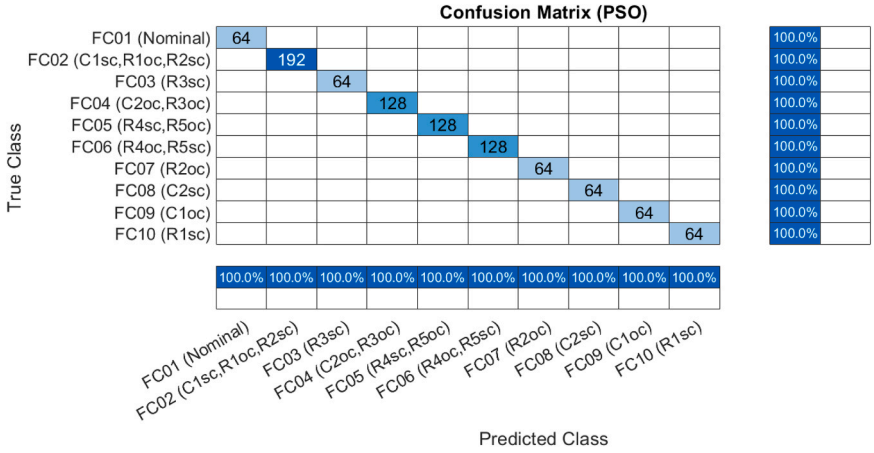

Fig. 13. Confusion matrix of the Sugeno FIS after using a PSO algorithm for predicting the faults using the Monte Carlo analysis data.

faults, but also those obtained from the Monte Carlo analysis so that it is possible to detect all of them.

Fig. 13 shows that all of the 960 possible events generated by the Monte Carlo analysis are now correctly classified, unlike what happened in the initial Sugeno FIS.

Moreover, as can be seen from the ROC curve, shown in Fig. 14, the FIS obtained in this way is a perfect classifier for this type of circuit. That is, all the fault classes are now correctly classified with the particle swarm optimization algorithm. Therefore, this adjusted FIS could be used to predict the faults in the filter. Likewise, Fig. 15 shows the performance of the adjusted FIS using the PSO method.

Although the PSO provided sufficiently accurate enough results, a pattern search optimization algorithm [31] was also used in this study to improve the results provided by the initial FIS. Fig. 16 shows the adjusted membership functions of the initial Sugeno FIS using this optimization algorithm.

Results of the adjusted FIS using a pattern search algorithm are shown in Figs. 17 and 18. In this case, it can be observed that the adjusted FIS is also able to accurately predict all the hard faults that can occur in the S-K filter.

Fig. 17 shows the confusion matrix and Fig. 18 depicts the performance of the adjusted FIS in predicting the 960 events obtained from the Monte Carlo analysis. As can be noted in Fig. 17 all the faults are correctly classified.

As shown in Fig. 14 and Fig. 19, a perfect classification is obtained from the initial Sugeno FIS using either a PSO or a pattern search optimization algorithm. As can be seen in these two figures, the ROC has an area under the curve (AUC) of one, which shows that the Sugeno FIS adjusted with either a PSO or a pattern search optimization algorithm is able to diagnose the operating modes of the S-K once they have been classified as shown in Table 4. As can be noted, although a 10%

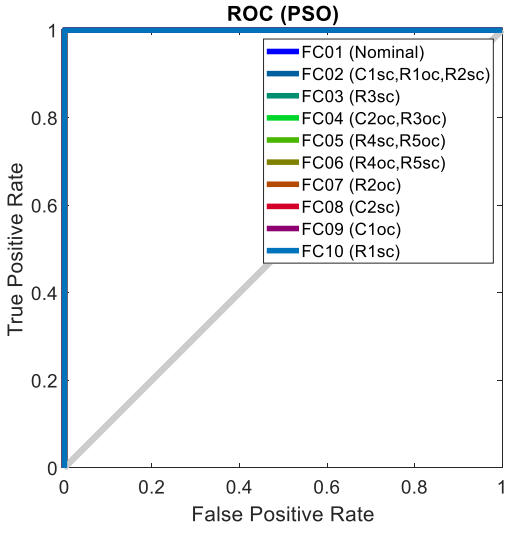

Fig. 14. ROC curve of the Sugeno FIS using particle swarm optimization (PSO).

tolerance in the components is a very high value for a filter, the tuned FISs were able to detect both the correct operating mode and the hard faults. It is worth mentioning that in this study the membership functions were modified, but the FIS outputs were kept at the values of the initial zero-order Sugeno FIS, which corresponded to the nominal behavior and fault classes.

The fitness function used to optimize the membership functions of the initial FIS was the root mean square error (RMSE). This fitness

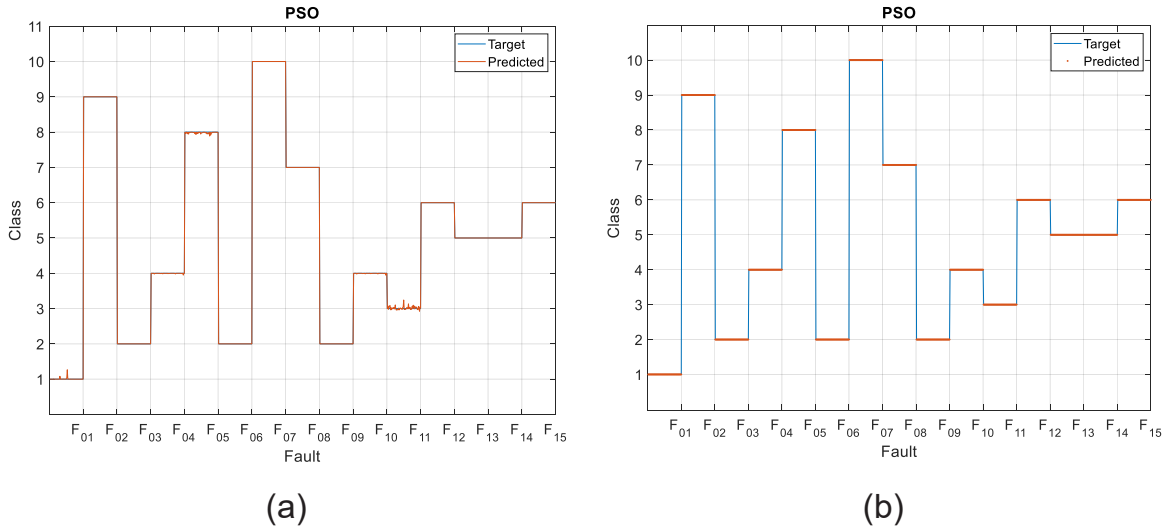

Fig. 15. Output of the tuned FIS using a PSO algorithm (a) actual output values and (b) output values rounded to the nearest integer.

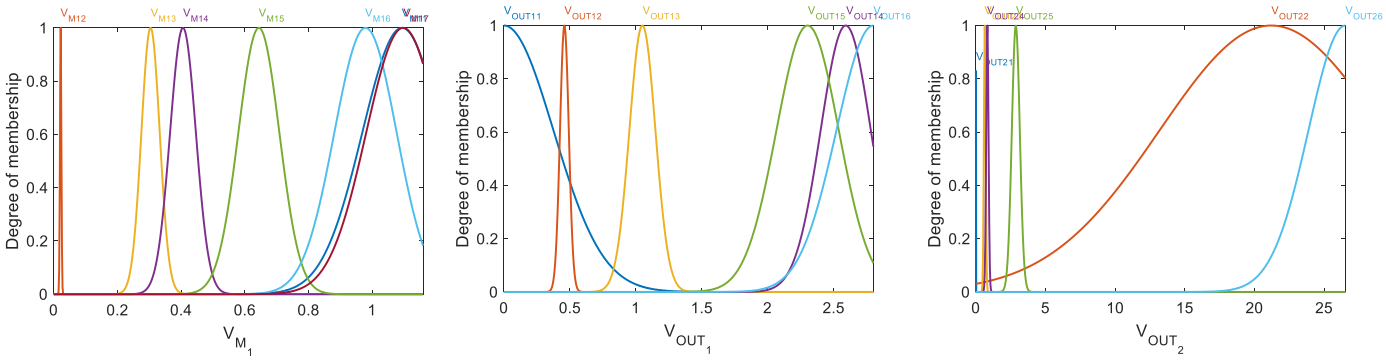

Fig. 16. Membership functions for classifying the faults in the S-K circuit using a pattern search optimization algorithm.

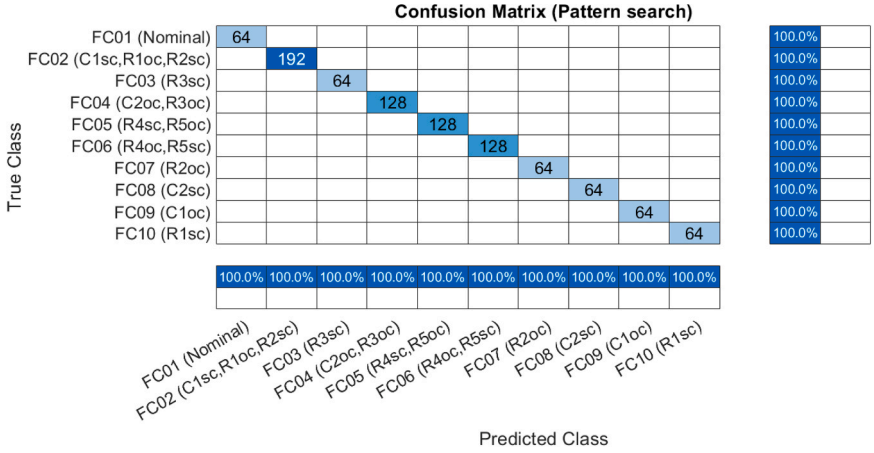

Fig. 17. Confusion matrix of the Sugeno FIS after using a pattern search optimization algorithm for predicting the faults using the data of the Monte Carlo analysis.

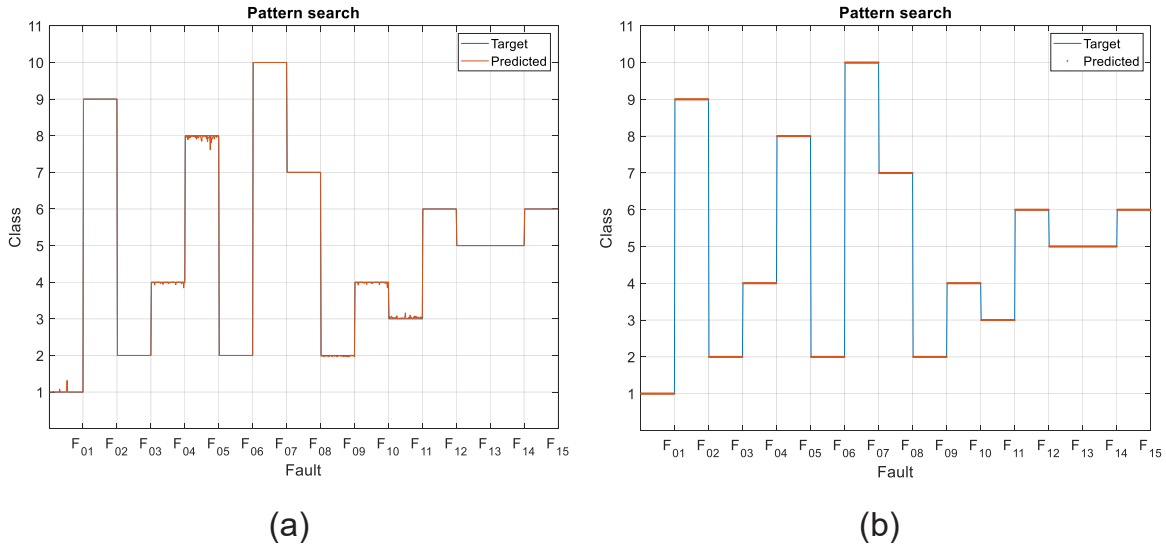

Fig. 18. Output of the tuned FIS using a pattern search optimization algorithm (a) actual output values and (b) output values rounded to the nearest integer.

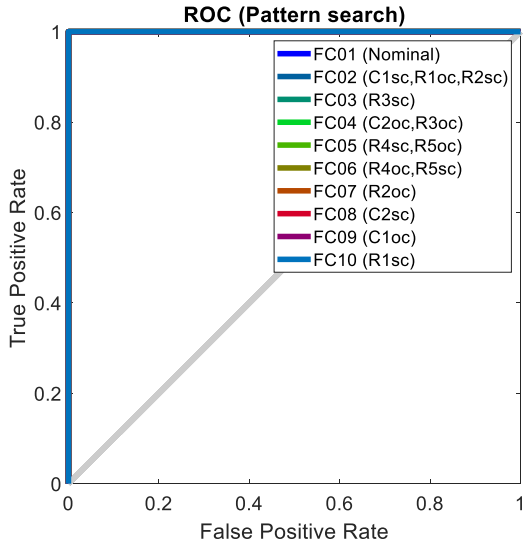

Fig. 19. ROC curve of the Sugeno FIS using pattern search optimization.

function is shown in Eq. (7) where y_j and $\hat{y}_j$ are the actual value and the estimated value using the tuned fuzzy inference system, respectively.

$$RMSE = \sqrt{\frac{1}{N}\sum_{j=1}^{N}\left(y_j - \hat{y}_j\right)^2} \tag{7}$$

Fig. 20 shows a comparison between the function values obtained, with a maximum number of iterations of 500, for the PSO and for the pattern search algorithms. Although both algorithms allow a complete fault classification to be obtained, as can be seen, the PSO provides better values than those obtained with the pattern search algorithm in terms of convergence and fitness values. Specifically, in the case of the pattern search, the best fitness value was 0.017073 after 500 iterations and that obtained in the case of the PSO was 0.001965. Therefore, the PSO value is much better than the one obtained with the pattern search method.

In this current study, a methodology based on fuzzy logic has been considered for fault detection. However, other techniques could also be used, such as those based on Artificial Neural Networks (ANN), as shown in Fig. 21, where a patternnet type ANN using a Levenberg-Marquardt

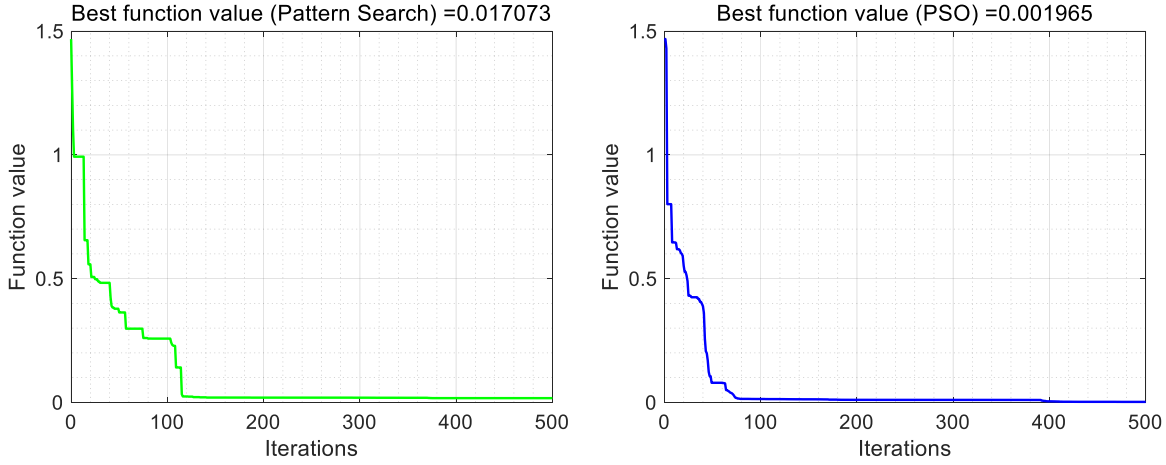

Fig. 20. Comparison of performance between PSO and pattern search algorithms.

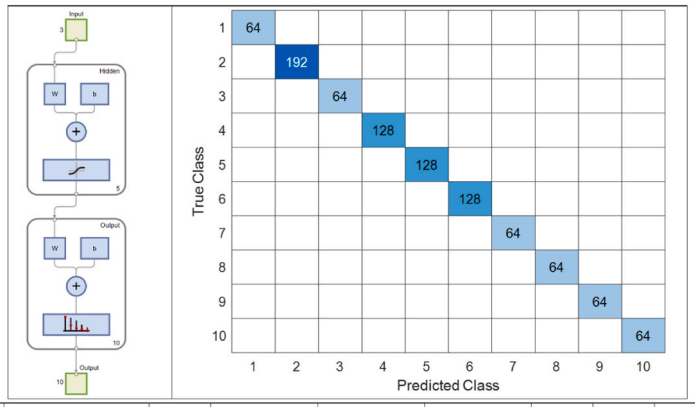

1	2	3	4	5	6	7	8	9	10
Nominal	{C_{1sc}, R_{1oc}, R_{2sc}}	R_{3sc}	{C_{2oc}, R_{3oc}}	{R_{4sc}, R_{5oc}}	{R_{4oc}, R_{5sc}}	R_{2oc}	C_{2sc}	C_{1oc}	R_{1sc}

Fig. 21. Results obtained with a patternnet ANN.

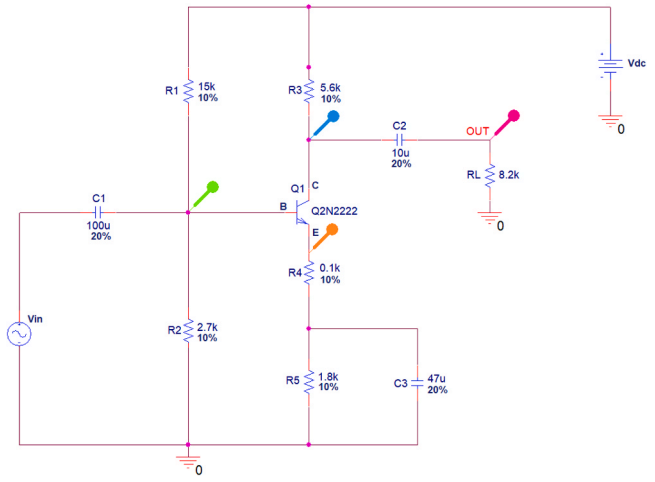

Fig. 22. Electrical diagram of the second circuit under test (CUT).

backpropagation algorithm, a hyperbolic tangent sigmoid transfer function in the hidden layer and a softmax function in the output were used to analyze the faults in the Sallen-Key. In this case, the same number of inputs as those employed in the FIS were selected from the output voltage, and from the M1 voltage with similar results to those shown previously with the FIS.

3.2. Analysis of a small signal BJT amplifier

This second CUT is a small signal BJT amplifier and is shown in Fig. 22, where the passive components have normalized values and are assumed to have tolerance of 10% for resistors and 20% for capacitors. From the analysis of the CUT shown in Fig. 22 it is possible to determine 14 individual hard faults in the passive components. Therefore, from the selected inputs (V_B, V_C, V_E, Av), i.e., DC voltages and gain voltage, it is possible to identify 11 fault classes that include faults with ambiguous configuration, since it is not possible to measure all circuit components from a practical point of view. Table 6 shows the hard faults and the faults classes identified [13].

From the analysis of the fault classes, eight membership functions were identified for the DC voltages (V_B, V_C, V_E) and six membership functions corresponding to the gain voltage (Av). First, a zero-order Sugeno FIS was developed from these Gaussian membership functions, where the FIS had eleven rules, each of them corresponding to the nominal behavior and to the fault classes shown in Table 6.

Using a procedure similar to the previous CUT, the initial FIS was developed from the actual hard faults where the membership employed were also Gaussians. Their mean values were taken from the average values within each fault class and their standard deviation was considered to be 10% of these nominal values. Furthermore, in this second case, when the mean was zero, a standard deviation of 0.1 was used. Fig. 23 shows the Gaussian membership functions employed, which were obtained from Eq. (6) by using the values given in Table 7.

Fig. 24 shows the rule inference of the Sugeno FIS developed to predict faults in the second CUT for the particular case of fault class number five, which is the open circuit in the C3 capacitor. As can be seen, the original Sugeno FIS was able to detect this fault. Moreover, this zero-order Sugeno FIS predicted 100% of the actual hard faults, i.e., when the passive components were in an actual short circuit or open circuit, which is logical since the FIS was developed from these situations. However, this initial FIS may not correctly predict other hard fault situations prior to the actual hard fault. Similar to the previous CUT, to validate the initial Sugeno FIS, a Monte Carlo analysis was performed from the tolerances of the resistors and capacitors of the circuit shown in Fig. 22. Fig. 25 shows the variability observed at the selected measurement points.

Fig. 26 shows the confusion matrix obtained with the initial fuzzy inference system for the second CUT. As can be observed, FC_{02} and FC_{08} are misclassified. Therefore, although the results provided by the FIS are

Table 6
Hard faults grouped by ambiguity groups and nominal behavior.

FC_{01}	FC_{02}	FC_{03}	FC_{04}	FC_{05}	FC_{06}	FC_{07}	FC_{08}	FC_{09}	FC_{10}	FC_{11}
F_{01}	F_{13}	{F_{02}, F_{05}, F_{11}}	{F_{10}, F_{12}}	F_{14}	{F_{09}, F_{15}}	F_{07}	F_{08}	F_{03}	F_{04}	F_{06}
Nominal	C_{2sc}	{R_{1oc}, R_{2sc}, C_{1sc}}	{C_{1oc}, C_{2oc}}	C_{3oc}	{R_{4sc}, C_{3sc}}	R_{3sc}	R_{4oc}	R_{1sc}	R_{2oc}	R_{3oc}

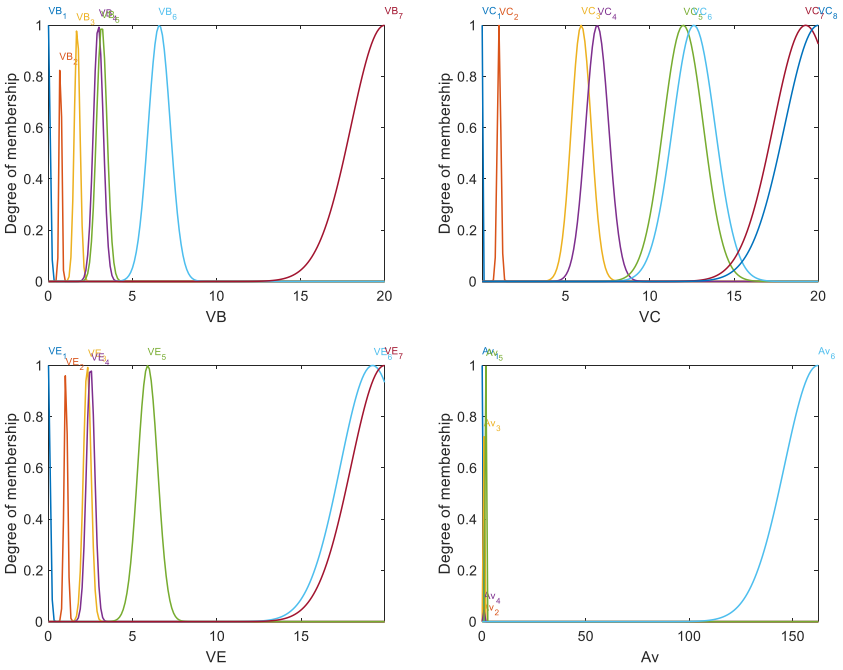

Fig. 23. Membership functions for modeling the faults in the BJT circuit.

Table 7
Fault classes for the small-signal BJT amplifier. (VB (V), VC (V), VE (V), Av).

Class	Fault	Name	VB	VBj	VC	VCj	VE	VEj	Av	Avj
FC01	F01	Nominal	2.939	4	12.61	6	2.272	3	162.225	6
FC02	F13	C_{2sc}	3.166	5	6.868	4	2.496	4	161.849	6
FC03	F02	R_{1oc}	0.000	1	20	8	0	1	0	1
FC03	F05	R_{2sc}	0.000	1	20	8	0	1	0	1
FC03	F11	C_{1sc}	0.000	1	20	8	0	1	0	1
FC04	F10	C_{1oc}	2.939	4	12.61	6	2.272	3	0	1
FC04	F12	C_{2oc}	2.939	4	12.61	6	2.272	3	0	1
FC05	F14	C_{3oc}	3.167	5	11.98	5	2.497	4	1.8181	5
FC06	F09	R_{4sc}	0.711	2	0.035	1	0	1	1.19943	4
FC06	F15	C_{3sc}	0.711	2	0.035	1	0	1	1.19943	4
FC07	F07	R_{3sc}	3.046	4	20	8	2.38	3	0	1
FC08	F08	R_{4oc}	2.955	4	20	8	19.95	7	0	1
FC09	F03	R_{1sc}	20.000	7	19.25	7	19.24	6	0	1
FC10	F04	R_{2oc}	6.594	6	5.92	3	5.889	5	0.9804	3
FC11	F06	R_{3oc}	1.703	3	1.037	2	1.027	2	0.068	2

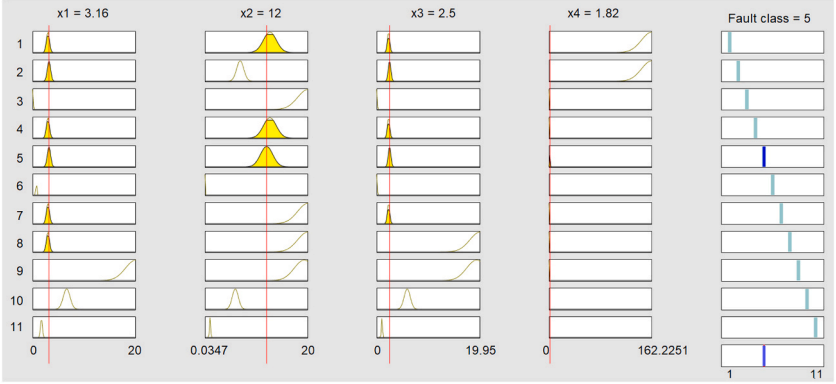

Fig. 24. Rule inference of the initial Sugeno FIS.

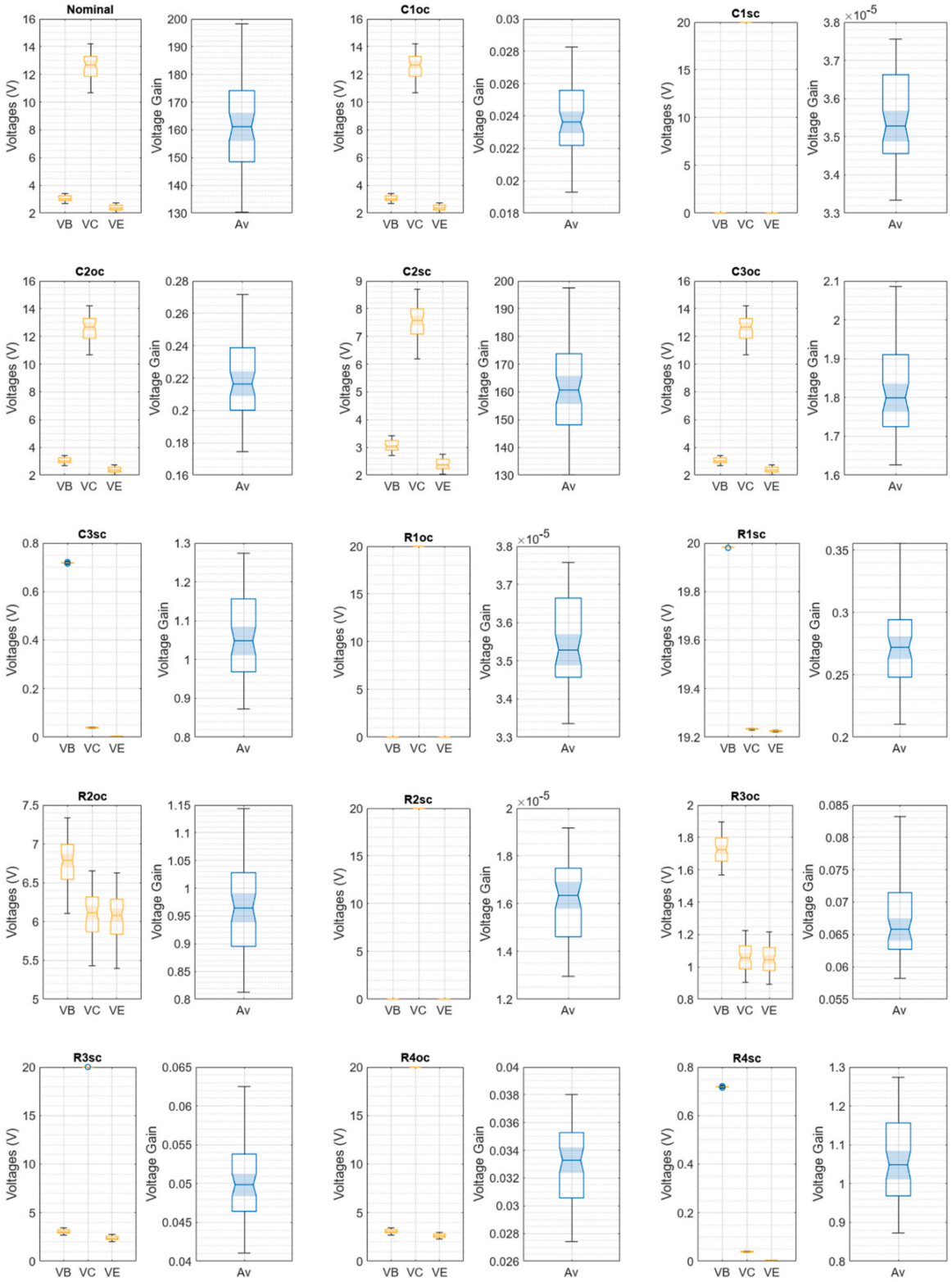

Fig. 25. Results of the Monte Carlo analysis from the tolerances of the resistors and capacitors of the circuit.

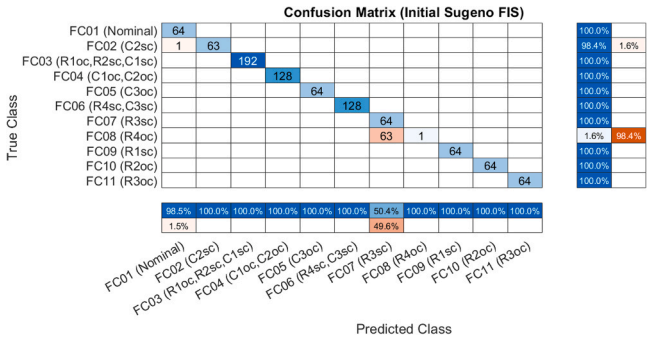

Fig. 26. Confusion matrix showing the performance of the initial zero-order Sugeno FIS for predicting faults in the 2nd CUT.

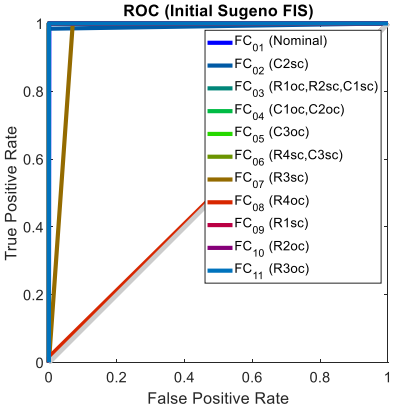

Fig. 27. ROC curve of the initial Sugeno FIS for the 2nd CUT.

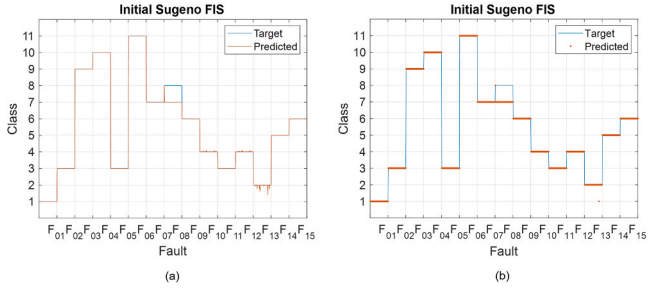

Fig. 28. Output of the initial Sugeno FIS for the 2nd CUT (a) actual output values and (b) output values rounded to the nearest integer.

reliable after the actual hard fault occurs, in situations prior to the actual hard fault it would not be possible to accurately detect all of them. This behavior can be observed in Fig. 27 and Fig. 28, which show the ROC curve and the outputs of the FIS, respectively.

In order to improve the results obtained with the initial FIS a pattern search algorithm was first used to adjust the membership functions of the initial FIS. These new adjusted membership functions are shown in Fig. 29.

Fig. 30 shows that the optimized FIS using a pattern search optimization algorithm does not significantly improve the results obtained with the initial Sugeno FIS. As can be observed, fault class $F_{07}(R_{3sc})$ and $F_{08}(R_{4oc})$ are still misclassified. The same can also be observed in both Fig. 31 and Fig. 32.

It can be seen that a pattern search optimization algorithm still

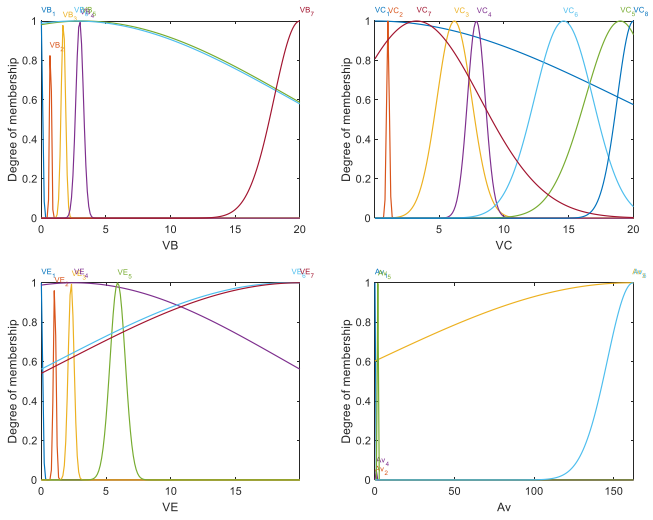

Fig. 29. Membership functions for classifying the faults in the BJT circuit after the pattern search optimization.

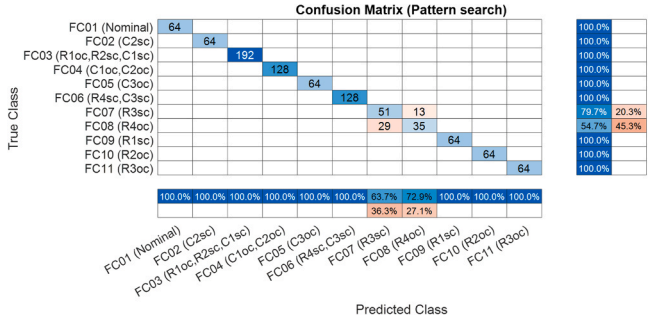

Fig. 30. Confusion matrix showing the performance of the adjusted FIS by using a pattern search optimization algorithm.

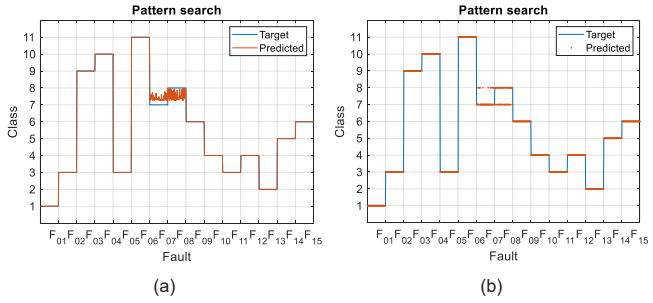

Fig. 31. Output of the adjusted FIS using a pattern search optimization algorithm (a) actual output values and (b) output values rounded to the nearest integer.

misclassifies some data of fault classes FC_7 and FC_8. Therefore, a second optimization algorithm is considered in order to increase the accuracy. Therefore, a particle swarm optimization algorithm [31] was also analyzed. Fig. 33 shows the membership functions adjusted with this algorithm. It should be noted that the same number of iterations was used for all optimization algorithms.

As shown in Figs. 34 and 35, 100% of the Monte Carlo results were now correctly classified by using PSO. The same can be seen in the ROC

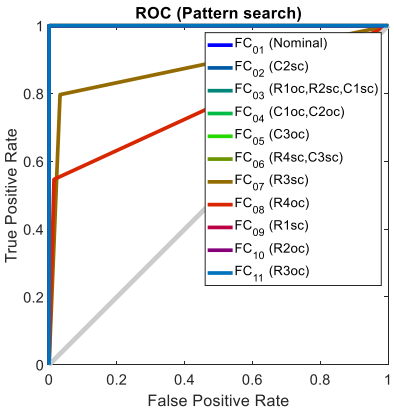

Fig. 32. ROC curve of the Sugeno FIS for the 2nd CUT using pattern search optimization.

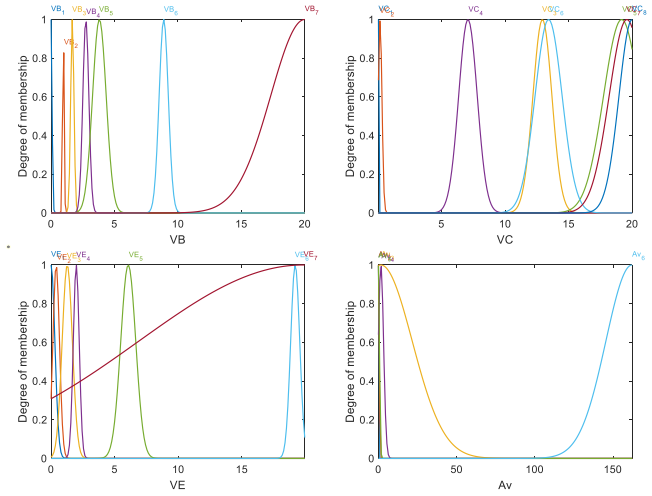

Fig. 33. Membership functions for classifying the faults in the BJT circuit after the PSO.

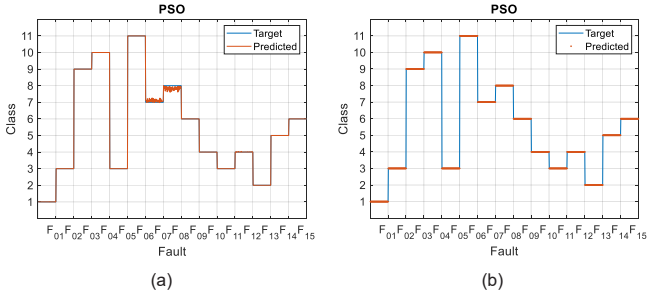

Fig. 34. Output of the adjusted FIS using a particle swarm optimization algorithm (a) actual output values and (b) output values rounded to the nearest integer.

curve shown in Fig. 36.

Fig. 36 shows that the ROC has an area under the curve (AUC) of one, which indicates that the Sugeno FIS adjusted with a particle swarm optimization algorithm was able to diagnose the faults and the nominal behavior of the BJT amplifier.

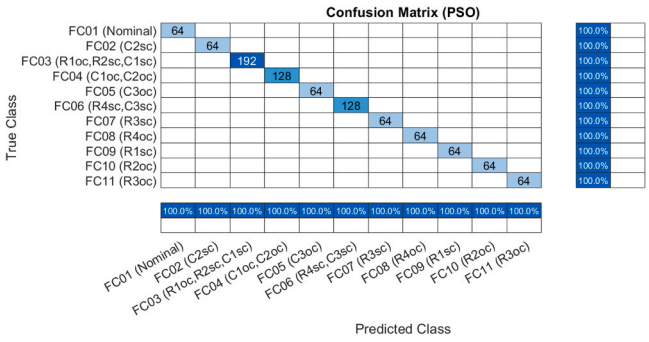

Fig. 35. Confusion matrix showing the performance of the adjusted FIS by using a particle swarm optimization algorithm.

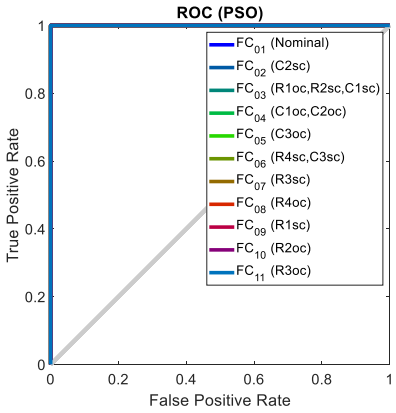

Fig. 36. ROC curve of the tuned FIS for predicting the faults using a particle swarm optimization algorithm.

4. Conclusions

In the present study, the application of a zero-order Sugeno FIS combined with different optimization algorithms based on particle swarm optimization and pattern search has been shown for the diagnosis of individual hard faults in two CUTs: a second-order bandpass Sallen-Key filter and a single stage of a small signal amplifier. The procedure to develop the initial Sugeno FIS from the actual individual hard faults was also shown. Likewise, how to optimize the membership functions to detect hard faults that may occur in these two analog electronic circuits was also discussed.

The fuzzy inference systems developed for hard fault detection in these CUTs have the advantage of having a reduced number of rules that were obtained from an analysis of actual hard faults that may occur in the circuits. In the case of the first CUT, it was shown that the initial Sugeno FIS was not able to accurately detect all the fault classes in the Sallen-Key filter. Only two fault classes were detected with 100% accuracy and only five of them were correctly predicted, i.e. there were no misclassified data, (FC_{09} and FC_{10}). Regarding the remaining fault classes, when FC_{03} occurred there were some other values that were also predicted as FC_{03} by the initial FIS and did not correspond to this class (63 values corresponding to FC_{02} class and 1 value of the nominal class were misclassified as FC_{03}). Similar behavior was observed for fault classes (FC_{05}, FC_{06}, FC_{07} and FC_{08}). However, when a PSO algorithm was used to adjust the membership functions of the initial Sugeno FIS, the AUC of the ROC curve was equal to one, which means that a perfect classification was obtained with this adjusted FIS to predict the faults that may occur in the circuit. Likewise, the same behavior was obtained

when a pattern search algorithm was used.

With regard to the application of the initial Sugeno FIS to the second CUT considered in this study a similar behavior was obtained, that is, although the initial Sugeno FIS was able to detect the actual hard faults, it was not able to accurately detect the previous events obtained from the Monte Carlo analysis. In this case, FC_{02} and FC_{08} were misclassified by the initial Sugeno FIS. Therefore, although the results provided by the FIS after the actual hard fault has occurred are reliable, in situations before the actual hard fault, it would not be possible to accurately detect all of them. In this case, the pattern search optimization algorithm did not show much improved results, but the use of a PSO led to a complete classification of the faults that may arise in the circuit. This means that 100% of the possible defects simulated by the Monte Carlo analysis were correctly detected by a particle swarm optimization algorithm.

This current study could be applied to fault detection in analog circuits similar to those shown in the manuscript, in order to determine hard faults that may occur in the passive components. As it has been shown, the proposed methodology allows these hard faults to be accurately determined. However, it should be mentioned that there may be some faults with similar output from the point of view of the measuring points, and therefore they should be previously identified in order to be able to apply the current method to fault detection in the analog circuits.

Declaration of Competing Interest

The author declares that she has no financial interests or personal relationships that could have influenced the work presented in this article.

References

[1] E. Afacan, N. Lourenço, R. Martins, G. Dündar, Review: machine learning techniques in analog/RF integrated circuit design, synthesis, layout, and test, Integration 77 (2021) 113–130, https://doi.org/10.1016/j.vlsi.2020.11.006.

[2] A.A.A. Mohd Amiruddin, H. Zabiri, S.A.A. Taqvi, L.D. Tufa, Neural network applications in fault diagnosis and detection: an overview of implementations in engineering-related systems, Neural Comput. Appl. 32 (2020) 447–472, https://doi.org/10.1007/s00521-018-3911-5.

[3] J. Gong, X. Yang, K. Qian, Z. Chen, T. Han, Application of improved bubble entropy and machine learning in the adaptive diagnosis of rotating machinery faults, Alex. Eng. J. 80 (2023) 22–40, https://doi.org/10.1016/j.aej.2023.08.006.

[4] W. Molla Salilew, Z. Ambri Abdul Karim, T. Alemu Lemma, Investigation of fault detection and isolation accuracy of different Machine learning techniques with different data processing methods for gas turbine, Alex. Eng. J. 61 (2022) 12635–12651, https://doi.org/10.1016/j.aej.2022.06.026.

[5] A. Arabi, M. Ayad, N. Bourouba, M. Benziane, I. Griche, S.S.M. Ghoneim, E. Ali, M. Elsisi, R.N.R. Ghaly, An efficient method for faults diagnosis in analog circuits based on machine learning classifiers, Alex. Eng. J. 77 (2023) 109–125, https://doi.org/10.1016/j.aej.2023.06.090.

[6] S. Qiu, X. Cui, Z. Ping, N. Shan, Z. Li, X. Bao, X. Xu, Deep learning techniques in intelligent fault diagnosis and prognosis for industrial systems: a review, Sensors 23 (2023), https://doi.org/10.3390/s23031305.

[7] L. Zuo, L. Hou, W. Zhang, S. Geng, W. Wu, Application of PSO-Adaptive Neural-fuzzy Inference System (ANFIS) in Analog Circuit Fault Diagnosis, in: Adv. Swarm Intell. First Int. Conf. ICSI 2010, Springer Berlin Heidelberg, 2010: pp. 51–57. https://doi.org/10.1007/978–3-642–13498-2_7.

[8] J. Shi, Y. Deng, Z. Wang, Analog circuit fault diagnosis based on density peaks clustering and dynamic weight probabilistic neural network, Neurocomputing 407 (2020) 354–365, https://doi.org/10.1016/j.neucom.2020.04.113.

[9] A. Zhang, C. Chen, B. Jiang, Analog circuit fault diagnosis based UCISVM, Neurocomputing 173 (2016) 1752–1760, https://doi.org/10.1016/j.neucom.2015.09.050.

[10] Y. Xiao, Y. He, A novel approach for analog fault diagnosis based on neural networks and improved kernel PCA, Neurocomputing 74 (2011) 1102–1115, https://doi.org/10.1016/j.neucom.2010.12.003.

[11] C. Zhang, Y. He, T. Yang, B. Zhang, J. Wu, An analog circuit fault diagnosis approach based on improved wavelet transform and MKELM, Circuits, Syst. Signal Process. 41 (2022) 1255–1286, https://doi.org/10.1007/s00034-021-01842-2.

[12] M. Sheikhan, A.A. Sha'bani, PSO-optimized modular neural network trained by OWO-HWO algorithm for fault location in analog circuits, Neural Comput. Appl. 23 (2013) 519–530, https://doi.org/10.1007/s00521-012-0947-9.

[13] M.I. Dieste-Velasco, Application of a pattern-recognition neural network for detecting analog electronic circuit faults, Mathematics 9 (2021) 3247, https://doi.org/10.3390/math9243247.

[14] T. Zhong, J. Qu, X. Fang, H. Li, Z. Wang, The intermittent fault diagnosis of analog circuits based on EEMD-DBN, Neurocomputing 436 (2021) 74–91, https://doi.org/10.1016/j.neucom.2021.01.001.

[15] I. Aizenberg, R. Belardi, M. Bindi, F. Grasso, S. Manetti, A. Luchetta, M.C. Piccirilli, A neural network classifier with multi-valued neurons for analog circuit fault diagnosis, Electronics 10 (2021) 349, https://doi.org/10.3390/electronics10030349.

[16] A. Arabi, N. Bourouba, A. Belaout, M. Ayad, An accurate classifier based on adaptive neuro-fuzzy and features selection techniques for fault classification in analog circuits, Integration 64 (2019) 50–59, https://doi.org/10.1016/j.vlsi.2018.08.001.

[17] A.R. Nasser, A.T. Azar, A.J. Humaidi, A.K. Al-Mhdawi, I.K. Ibraheem, Intelligent fault detection and identification approach for analog electronic circuits based on fuzzy logic classifier, Electronics 10 (2021) 2888, https://doi.org/10.3390/electronics10232888.

[18] W. He, Y. He, B. Li, C. Zhang, Feature extraction of analogue circuit fault signals via cross-wavelet transform and variational Bayesian matrix factorisation, IET Sci. Meas. Technol. 13 (2019) 318–327, https://doi.org/10.1049/iet-smt.2018.5432.

[19] Y. Cui, J. Shi, Z. Wang, Analog circuit fault diagnosis based on Quantum Clustering based Multi-valued Quantum Fuzzification Decision Tree (QC-MQFDT), Measurement 93 (2016) 421–434, https://doi.org/10.1016/j.measurement.2016.07.018.

[20] X. Li, Y. Xie, Analog circuits fault detection using cross-entropy approach, J. Electron. Test. 29 (2013) 115–120, https://doi.org/10.1007/s10836-012-5344-x.

[21] W. He, Y. He, B. Li, C. Zhang, Analog circuit fault diagnosis via joint cross-wavelet singular entropy and parametric t-SNE, Entropy 20 (2018) 1–20, https://doi.org/10.3390/e20080604.

[22] J. Yang, T. Gao, S. Jiang, A dual-input fault diagnosis model based on SE-MSCNN for analog circuits, Appl. Intell. 53 (2023) 7154–7168, https://doi.org/10.1007/s10489-022-03665-3.

[23] H.M. Khalid, S.Z. Rizvi, L. Cheded, R. Doraiswami, A. Khoukhi, A PSO-Trained Adaptive Neuro-Fuzzy Inference System for Fault Classification, in: Proc. Int. Conf. Fuzzy Comput. 2nd Int. Conf. Neural Comput., SciTePress - Science and and Technology Publications, 2010: pp. 399–405. https://doi.org/10.5220/0003072303990405.

[24] A. Kumar, A.P. Singh, Fuzzy classifier for fault diagnosis in analog electronic circuits, ISA Trans. 52 (2013) 816–824, https://doi.org/10.1016/j.isatra.2013.06.006.

[25] W. Yu, Y. Sui, J. Wang, The faults diagnostic analysis for analog circuit based on FA-TM-ELM, J. Electron. Test. 32 (2016) 459–465, https://doi.org/10.1007/s10836-016-5597-x.

[26] M. Parai, S. Srimani, K. Ghosh, H. Rahaman, Multi-source data fusion technique for parametric fault diagnosis in analog circuits, Integration 84 (2022) 92–101, https://doi.org/10.1016/j.vlsi.2022.01.005.

[27] W. He, Y. He, Q. Luo, C. Zhang, Fault diagnosis for analog circuits utilizing time-frequency features and improved VVRKFA, Meas. Sci. Technol. 29 (2018), https://doi.org/10.1088/1361-6501/aaa33a.

[28] P. Bilski, Hierarchical diagnostics of analog systems based on the ambiguity groups detection, Measurement 119 (2018) 1–10, https://doi.org/10.1016/j.measurement.2018.01.029.

[29] G. Zhao, X. Liu, B. Zhang, Y. Liu, G. Niu, C. Hu, A novel approach for analog circuit fault diagnosis based on deep belief network, Measurement 121 (2018) 170–178, https://doi.org/10.1016/j.measurement.2018.02.044.

[30] D. Binu, B.S. Kariyappa, A survey on fault diagnosis of analog circuits: Taxonomy and state of the art, AEU Int. J. Electron. Commun. 73 (2017) 68–83, https://doi.org/10.1016/j.aeue.2017.01.002.

[31] The MathWorks Inc, Fuzzy Logic Toolbox™ User's Guide © Copyright 1995–2022 by The MathWorks, Inc., 2022.

[32] T. Takagi, M. Sugeno, Fuzzy identification of systems and its applications to modeling and control, IEEE Trans. Syst. Man. Cybern. SMC 15 (1985) 116–132, https://doi.org/10.1109/TSMC.1985.6313399.

[33] J.M. Mendel, Uncertain Rule-Based Fuzzy Systems, Springer International Publishing, Cham, 2017, https://doi.org/10.1007/978-3-319-51370-6.

[34] M. Versaci, S. Calcagno, M. Cacciola, F.C. Morabito, I. Palamara, D. Pellicanò, Standard soft computing techniques for characterization of defects in nondestructive evaluation. in: Ultrason. Nondestruct. Eval. Syst, Springer International Publishing, Cham, 2015, pp. 175–199, https://doi.org/10.1007/978-3-319-10566-6_6.

[35] J. Kennedy, R. Eberhart, Particle swarm optimization, in: Proc. ICNN'95 - Int. Conf. Neural Networks, IEEE, 2010: pp. 1942–1948. https://doi.org/10.1109/ICNN.1995.488968.

[36] The MathWorks Inc, Global Optimization Toolbox™ User's Guide ©Copyright 2004–2022 by The MathWorks, Inc., 2022.

[37] M. Cacciola, S. Calcagno, F.C. Morabito, M. Versaci, Swarm optimization for imaging of corrosion by impedance measurements in eddy current test, IEEE Trans. Magn. 43 (2007) 1853–1856, https://doi.org/10.1109/TMAG.2007.892513.